

Evidence for nonequilibrium dynamics and an overlap length scale in a reentrant (Fe_{0.65}Ni_{0.35})_{0.882}Mn_{0.118} ferromagnet

D. Li, R. M. Roshko, and G. Yang

Department of Physics, University of Manitoba, Winnipeg, Manitoba, Canada R3T2N2

(Received 27 July 1993)

The relaxation of the low-field thermoremanent magnetization has been measured, as a function of temperature and system age, for a reentrant (Fe_{0.65}Ni_{0.35})_{1-x}Mn_x ferromagnet with $x=0.118$. A dynamic crossover is observed in the vicinity of the reentrant transition from a high-temperature ($T \geq 65$ K) regime of equilibrium dynamics, where the relaxation isotherms are compatible with a weak power law, and exhibit no measurable dependence on system age, to a low-temperature ($T \leq 60$ K) regime, where the isotherms exhibit an age dependence symptomatic of nonequilibrium dynamics, and are describable analytically by a stretched exponential. Moreover, temperature-cycling experiments clearly confirm the instability of this low-temperature reentrant phase to variations in temperature, and thus support the existence of an overlap length scale, which is regarded by droplet scaling theories as a defining feature of the spin-glass state. The data are compared with the functional forms predicted by various phenomenological models of relaxation dynamics in systems with randomness.

INTRODUCTION

One of the most distinctive features of the spin-glass state is its extremely slow approach to equilibrium: if a spin glass is cooled rapidly through its ordering temperature T_{SG} to some temperature $T < T_{SG}$, and then probed after waiting for a time t_w at constant T , the relaxation response is observed¹ to vary with the age of the system, as measured by the wait time t_w , indicating that true equilibrium is never established on normal laboratory time scales ($t_{obs} < 10^5$ s). According to the phenomenological nearest-neighbor Ising model of Fisher and Huse,² which is based on a number of postulates regarding the nature and energetics of the elementary (droplet) excitations of the spin-glass state, this behavior is a consequence of the slow, logarithmic, barrier-activated growth of the spin-glass domains with time, $R(t) \sim (T \ln t)^{1/\psi}$, coupled with the extreme fragility of the spin-glass state to arbitrarily small variations in temperature ΔT , which causes the domain structure to fracture on length scales greater than the overlap length $l_{\Delta T} \sim |\Delta T|^{-\zeta}$. The model predicts a crossover at observation times $t \sim t_w$ from a regime of quasiequilibrium magnetization decay, $m(t) \sim (\ln t)^{-\theta/\psi}$, valid for $\ln t \ll \ln t_w$, to a regime of faster, nonequilibrium decay, $m(t) \sim (\ln t)^{-\lambda/\psi}$ with $\lambda > \theta$, valid for $\ln t \gg \ln t_w$. A similar approach due to Koper and Hilhorst,³ which postulates that a nonequilibrium spin glass in a field H at a temperature T may be decomposed into a network of finite (T', H') domains for any arbitrary pair (T', H') , which grow and fracture according to specific rules but which may never exceed the overlap length $l(T' - T, H' - H) \sim |\Delta T|^{-\zeta} |\Delta H|^{-\zeta'}$, also yields a crossover from slow, power-law, equilibrium dynamics to a more rapid, nonequilibrium, stretched-exponential-like decay in response to a small probing field:

$$M(t) = M_i \left[1 + \frac{t}{t_0} \right]^{-\alpha} \times \left\{ \exp - \frac{t_2^n}{t_1(1-n)} [(t + t_w)^{1-n} - t_w^{1-n}] \right\}, \quad (1)$$

where t_0 , t_1 , and t_2 are temperature-dependent microscopic times.

Until very recently, alternative theoretical approaches, such as that of DeDominicis, Orland, and Lainée,⁴ based on the mean-field solution⁵ of the long-range Sherrington and Kirkpatrick (SK) Ising model,⁶ with its complex broken ergodicity and its infinity of quasidegenerate pure equilibrium states, have failed to replicate the aging phenomenon, although they have shown that the populations of a system of states with independent, random free energies exhibit a stretched-exponential approach to equilibrium. However, Bouchaud⁷ has developed a phenomenological theory of SK dynamics which links the aging of a field-cooled system to the multitude of accessible metastable magnetized states which tend to trap the system in local energy minima as it evolves towards "true" equilibrium, and to their broad distribution of lifetimes τ , which is required to have a divergent mean value $\langle \tau \rangle$ (this is termed "weak ergodicity breaking"). In essence, the realization that the deepest accessible minimum which is encountered traps the system for a time τ_{max} comparable to the overall wait time and that its properties thus dominate the system observables, coupled with the expectation that, when the field is switched off after waiting for a time t_w , the system may, with finite probability, continue to age by probing deeper and deeper magnetized wells before relaxing towards zero-magnetization states, leads rather naturally to an observation time-dependent age $t_a = t_w + t$, and to an explicitly wait-time-dependent decay of the form:

$$M(t) = M_i \exp\left[-\gamma \int_0^t t^{-x}(t+t_w)^{x-1} dt\right]. \quad (2)$$

Thus this model also features a crossover between two asymptotic relaxation regimes: a short-time ($t \ll t_w$) stretched-exponential response,⁷ due to aging in the field, and a long-time ($t \gg t_w$) power-law response,⁷ due to aging during relaxation.

Chamberlin and Haines⁸ have adopted a considerably more general approach, pointing out that the “universality” of the empirical functions used to characterize relaxation dynamics in random systems suggests a fundamental link to elementary excitations, and have proposed a model for activated relaxation of finite-size-quantized magnons within a *fixed*, percolation distribution of finite mesoscopic domains, in which domain rotation and wall motion play no role. In this model, a domain is defined as a region of dynamically correlated spins, where the spins all share a common relaxation rate, which varies exponentially with inverse domain size s , $\omega = \omega_\infty e^{\pm C/s}$, where s is the number of spins in the domain, and ω_∞ is the relaxation rate of an infinite domain. Percolation theory provides a specific prediction⁹ for the domain-size distribution, $n_s \sim s^{-\theta} \exp(-s^\delta)$, with exponent values $\theta = -\frac{1}{9}$ and $\delta = \frac{2}{3}$, which, when combined with the exponential temporal decay typical of barrier-activated dynamics, yields two mesoscopically exact relaxation functions,

$$M_\pm(t) = M_i \int_0^\infty x^{10/9} \exp(-x^{2/3}) \exp(-t\omega_\infty^\pm e^{\pm C/x}) dx, \quad (3)$$

for domains aligned (−) or antialigned (+) with the external field.

While the relaxation response of pure spin glasses has been the focus of extensive investigation, comparatively little attention has been devoted to random-exchange ferromagnets, particularly in their “reentrant” configuration,¹⁰ where the ferromagnetic (F) state supposedly collapses at low temperatures into a mixed ferromagnetic–spin-glass (FSG) ground state. This is somewhat surprising, since the validity of this sequential F→FSG picture is still a matter of considerable dispute, and relaxation experiments are expected to offer definitive evidence for such a spin rearrangement. In this paper, we present superconducting quantum interference device (SQUID) measurements of the low-field thermoremanent relaxation of a reentrant $(\text{Fe}_{0.65}\text{Ni}_{0.35})_{1-x}\text{Mn}_x$ ferromagnet with $x=0.118$, over four decades of observation time ($2 \leq t \leq 10^4$ s), and over a temperature interval spanning the entire ordered phase, which show that the ferromagnetic and reentrant phases are dynamically distinct, and that the latter possesses the defining features of the spin-glass state, as expressed by short-range droplet fluctuation theories.² The details of the magnetic phase diagram of this ternary system are well established,¹¹ and the choice of this particular composition was influenced by the dynamic-susceptibility studies of Hesse and co-workers,¹² which, for similar values of x , exhibit all the structural features symptomatic of a reentrant sequence.

EXPERIMENTAL DETAILS

An alloy of $(\text{Fe}_{0.65}\text{Ni}_{0.35})_{1-x}\text{Mn}_x$ with composition $x=0.118$ was prepared by arc-melting the appropriate amounts of 99.999% pure Fe (Johnson-Matthey Chemicals, England), 99.99% pure Ni (Johnson-Matthey), and 99.98% pure Mn flake (Aldrich Chemical Co., Milwaukee) on the water-cooled copper hearth of a titanium-gettered argon arc furnace using a tungsten electrode. The alloy was repeatedly inverted and remelted in order to ensure a homogeneous consistency, and melting losses were traced almost exclusively to Mn vaporization. A portion of the original ingot was cold rolled into a thin sheet, and a long thin needle-shaped sample with dimensions $8.14 \times 0.36 \times 0.24$ mm³ was cut from the sheet. (Magnetization measurements performed subsequently on other samples cut from widely different locations on the same sheet yielded very reproducible results, thus confirming the uniformity of composition of the ingot.) The needle was encapsulated in a quartz tube in an argon atmosphere, annealed for 4d at 920°C and then quenched rapidly into water. The static-magnetization and remanent-relaxation measurements were performed with a variable-temperature, variable-frequency SQUID susceptometer, which has been described in detail elsewhere in the literature.¹³

DATA ANALYSIS AND DISCUSSION

Figure 1 shows the temperature dependence of the static magnetization of the $(\text{Fe}_{0.65}\text{Ni}_{0.35})_{0.882}\text{Mn}_{0.118}$ sample measured under both field-cooled (FC) and zero-field-cooled (ZFC) conditions, in a static applied field $H_a = 1.0$ Oe. The profile is very similar to that observed in other reentrant versions of this system,¹⁴ and is also consistent with the magnetic phase diagram,¹¹ which predicts a Curie temperature $T_C \cong 150$ K and a reentrant temperature $T_R \cong 70$ K for this composition (vertical arrows in Fig. 1). For all temperatures $T < 160$ K, $M_{\text{FC}}(T) > M_{\text{ZFC}}(T)$, indicating the presence of significant irreversibility

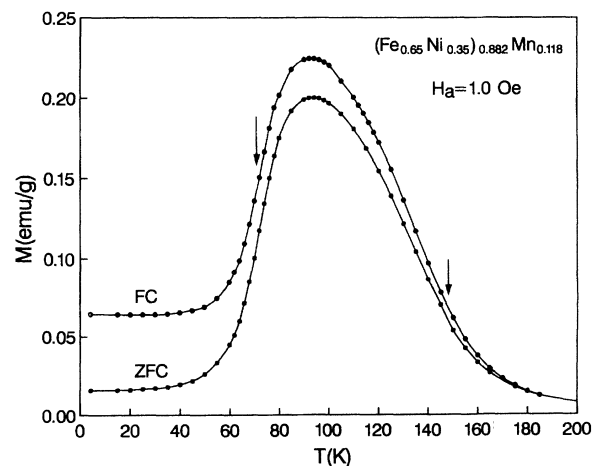


FIG. 1. Temperature dependence of the static magnetization of the $(\text{Fe}_{0.65}\text{Ni}_{0.35})_{1-x}\text{Mn}_x$ sample with $x=0.118$ measured under both field-cooled (FC) and zero-field-cooled (ZFC) conditions in a field $H_a = 1.0$ Oe.

TABLE I. Best-fit parameters to the stretched exponential in Eq. (4).

T_m (K)	t_w (s)	M_0 (10^{-3} emu/g)	M_i (10^{-3} emu/g)	n	τ (s)
40	60	117.90±0.05	15.10±0.06	0.650±0.005	$(2.83±0.05) \times 10^3$
45	60	110.70±0.08	22.90±0.10	0.680±0.005	$(2.12±0.04) \times 10^3$
50	60	101.90±0.11	34.50±0.16	0.730±0.003	$(1.37±0.02) \times 10^3$
52	60	97.30±0.09	39.30±0.16	0.740±0.005	$(8.56±0.09) \times 10^2$
55	60	87.80±2.70	51.00±0.28	0.790±0.005	$(3.57±0.03) \times 10^2$
57	60	85.30±0.15	60.90±0.43	0.820±0.005	$(1.62±0.02) \times 10^2$
57	300	86.00±0.16	58.00±0.36	0.810±0.005	$(3.13±0.04) \times 10^2$
57	900	82.40±0.18	62.30±0.33	0.830±0.005	$(6.42±0.10) \times 10^2$
57	3 600	73.80±0.35	72.60±0.53	0.850±0.005	$(3.09±0.13) \times 10^3$
57	10 800	58.00±2.00	89.50±2.59	0.880±0.005	$(2.89±0.70) \times 10^4$
60	60	81.80±0.08	84.80±0.42	0.870±0.005	23.4±0.5

throughout the entire ordered phase.

Figure 2 shows the decay of the thermoremanent magnetization at a sequence of measurement temperatures in the range $40 \leq T_m \leq 110$ K, and with a common experimental age, plotted on a logarithmic time scale. Each relaxation isotherm was obtained by cooling the sample in an applied field $H_c = 5.0$ Oe from a reference temperature $T_{\text{ref}} = 160$ K in the paramagnetic regime, where relaxation effects were negligible, to the measurement temperature T_m (the cooling procedure was very reproducible and yielded cooling times consistently close to $t_c = 900$ s), then abruptly removing the applied field and recording the decay over four decades of observation time $2 \leq t \leq 10^4$ s. These isotherms can be grouped into two distinct thermal regimes with completely different relaxation characteristics:

(a) For temperatures $T_m \leq 60$ K [Fig. 2(a)], which corresponds closely to the reentrant phase, the relaxation isotherms all exhibit a shape which may be described qualitatively as some portion of an S-shaped curve with an inflection point (vertical arrows), and quantitatively by the superposition of a stretched exponential and a constant:

$$M_R(t) = M_0 + M_i \exp[-(t/\tau)^{1-n}]. \quad (4)$$

This empirical representation, which is frequently invoked in analyses of pure spin-glass relaxation,¹⁵ provides an excellent description of the experimental data over the entire observation window [solid curves in Fig. 2(a)]. The best-fit values of the parameters n and τ listed in Table I are indeed typical of pure spin glasses; in particular, the exponent n increases with increasing temperature, and the trend towards unity indicates that the system is approaching its glass temperature. The necessity to supplement the stretched exponential with a substantial baseline term M_0 , which accounts for approximately 90–95 % of the entire remanent signal, is consistent with vector spin models of bond-disordered systems,¹⁶ which predict a longitudinal ferromagnetic spontaneous magnetization to coexist with transverse spin-glass freezing. Furthermore, the relaxation response in this regime is *not unique*, but rather exhibits a dependence on system age (t_w) which indicates that the low-temperature phase is a *nonequilibrium*

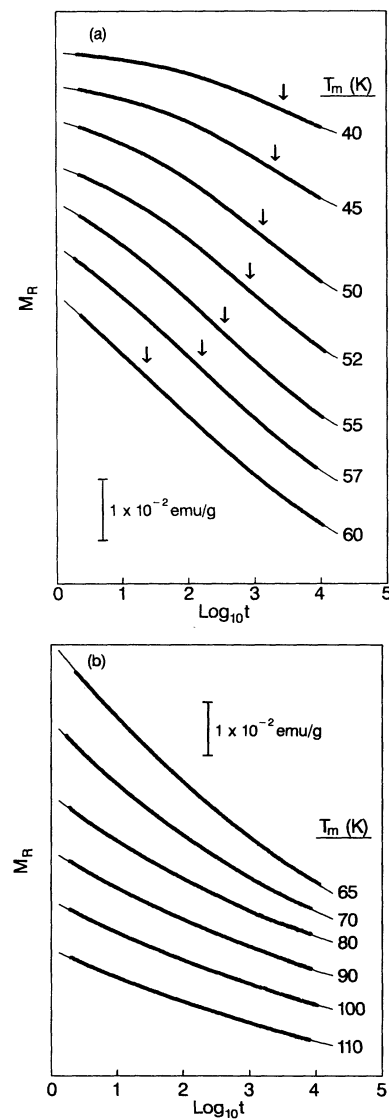


FIG. 2. (a) Thermoremanent relaxation isotherms for a sequence of temperatures $T_m \leq 60$ K and for a common wait time $t_w = 60$ s. The solid curves are fits to Eq. (4) and vertical arrows mark the characteristic times (inflection points) τ . (b) Thermoremanent relaxation isotherms for a sequence of temperatures $T_m \geq 65$ K and for a common wait time $t_w = 60$ s. The solid curves are fits to Eq. (5).

um phase. This is illustrated in Fig. 3 for a typical measurement temperature $T_m = 57$ K and for a sequence of wait times in the range $60 \leq t_w \leq 10800$ s; the effect is clearly visible in the relaxation rate $S(t) \equiv -\partial M_R(t)/\partial \ln t$, shown in Fig. 3(b), as a propagation of the inflection point towards longer observation times with increasing system age. The solid curves in Fig. 3(a) are best fits to Eq. (4), and an inspection of the corresponding parameters in Table I confirms that the aging process primarily affects the location of the inflection point (τ), without significantly altering the overall shape (n), at least for wait times $t_w \leq 10^4$ s.

(b) Over the temperature interval $65 \leq T_m \leq 160$ K, which is essentially coincident with the ferromagnetic phase, the curvature of the relaxation isotherms is uniformly positive [Fig. 2(b)], and all are accurately described by an empirical function consisting of the superposition of a simple power law and a constant (solid curves):

$$M_R(t) = M_0 + M_i t^{-m}, \quad (5)$$

with best-fit parameters listed in Table II. The functional form of the decay and the values of the exponent m are both typical of glassy relaxation dynamics in the extreme equilibrium limit of infinite age.¹⁷ In fact, in contrast to the reentrant phase, the isotherms in this regime exhibit *no* measurable dependence on system age, for wait times $t_w \leq 10^4$ s, indicating that, within the slow-cooling constraints of the current investigation, equilibrium is established far more rapidly in the high-temperature phase. This behavior is also consistent with that observed in “good” random ferromagnets, like $\text{Pd}_{0.986}\text{Fe}_{0.014}$,¹⁸ which is not reentrant and has “ideal” Heisenberg critical exponents, and with the droplet fluctuation model of Huse and Fisher, which predicts¹⁹ a power-law decay of the average temporal autocorrelation function in Ising ferromagnets with quenched bond disorder.

While the observation of a thermally driven crossover from equilibrium to nonequilibrium relaxation dynamics certainly offers compelling preliminary support for an orientational collapse from parallel to random spin alignment, it does not constitute conclusive evidence for genuine spin-glass freezing, since aging is also a feature of other types of systems, such as amorphous polymers,²⁰ high- T_c superconductors,²¹ and charge-density waves.²² However, as mentioned earlier, the spin-glass state exhibits a unique sensitivity to temperature, so that neighboring states at temperatures T and $T + \Delta T$ share nearly identical equilibrium spin correlations $\langle S_i \cdot S_j \rangle_T$ only up

TABLE II. Best-fit parameters to the power law in Eq. (5).

T_m (K)	t_w (s)	M_0 (10^{-3} emu/g)	M_i (10^{-3} emu/g)	m
65	60	55.40±0.30	63.80±0.28	0.072±0.001
70	60	73.40±0.10	43.80±0.10	0.088±0.001
80	60	85.90±0.19	34.10±0.18	0.082±0.001
90	60	95.00±0.14	33.60±0.13	0.066±0.001
100	60	97.70±0.12	29.80±0.12	0.064±0.001
110	60	90.90±0.15	27.70±0.14	0.060±0.001

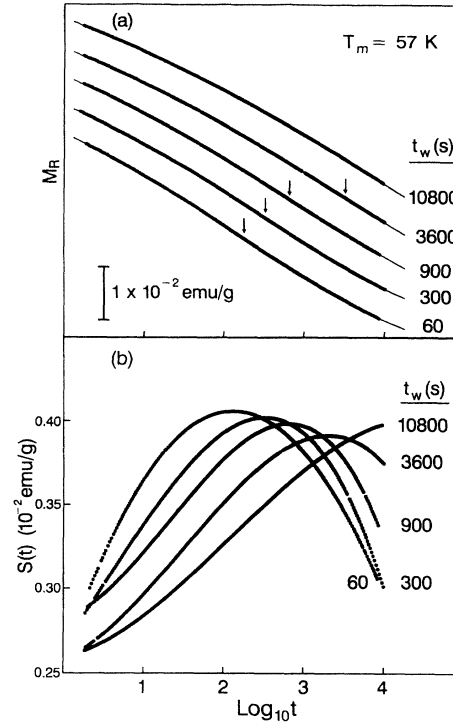


FIG. 3. (a) Wait-time dependence of the thermoremanent relaxation at $T = 57$ K. The solid curves are fits to Eq. (4), and the vertical arrows mark the inflection points τ . (b) The relaxation rate $S(t)$ for the isotherms in (a).

to the overlap length $l_{\Delta T}$, beyond which the signs of the correlations at T are uncorrelated with those at $T + \Delta T$. Temperature-cycling experiments provide a particularly direct method of detecting the overlap length through the limitations it imposes on the growth of spin-glass domains. If a spin glass is field cooled to a temperature T_m and, after a wait time t_w has elapsed, is subjected to a brief temperature cycle $T_m \rightarrow T_m + \Delta T \rightarrow T_m$, of duration $t_{\text{cycle}} \ll t_w$, immediately prior to field removal, then the subsequent behavior depends on the magnitude of ΔT as follows: (a) If $\Delta T < \Delta T_{\text{threshold}}$ then $l_{\Delta T} > R_T(t_w)$ (the overlap length is larger than the typical domain size at T_m), and there is only one type of domain and hence one maximum in the relaxation rate $S(t)$ at $t \sim t_w$. (b) If $\Delta T > \Delta T_{\text{threshold}}$, then $l_{\Delta T} < R_T(t_w)$ and some of the T_m domains will fracture into smaller ($T_m + \Delta T$) domains of dimension $l_{\Delta T}$, so $S(t)$ will exhibit two maxima at $t \sim t_{\text{cycle}}$ and $t \sim t_w$, corresponding to the two distinct domain sizes. (c) If $\Delta T \gg \Delta T_{\text{threshold}}$, virtually all the T_m domains will be annihilated, and there will be one maximum in $S(t)$ at $t \sim t_{\text{cycle}}$ due to the ($T_m + \Delta T$) domains alone.

Figure 4 shows the results of such a temperature-cycling experiment performed at a measurement temperature $T_m = 58$ K within the *reentrant* phase for $t_w = 10^4$ s, $t_{\text{cycle}} = 300$ s, and temperature increments ΔT listed in the figure. The curves labeled $\Delta T = 0$ and ∞ represent the two extreme single-domain configurations, the former with a single maximum at $t_m \cong 10^4$ s due to the large domains only, and the latter, which was obtained by heat-

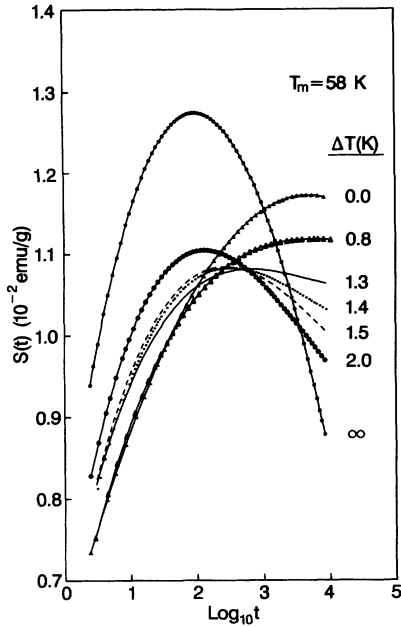


FIG. 4. The relaxation rate $S(t)$ measured at $T_m = 58$ K, after an initial waiting period $t_w = 10^4$ s at T_m followed by a temperature cycle $T_m \rightarrow T_m + \Delta T \rightarrow T_m$ of approximate duration $t_{\text{cycle}} = 300$ s. Note that the disappearance of one maximum is accompanied by the simultaneous growth of the other.

ing above the Curie temperature T_c , then cooling and aging for $t_w \cong t_{\text{cycle}}$ at T_m , also with a single maximum, but at $t_m \cong 300$ s due to the small domains only. For intermediate values of ΔT , the isotherms evolve systematically between these two limits and exhibit behavior which is consistent with a coexistence of the two types of domains; thus a weakening of one of the component maxima (reflecting a decline in the corresponding population) is invariably accompanied by an enhancement of the other. (The absence of multiple maxima in any of the intermediate isotherms is not entirely unexpected in reentrant systems, particularly ferromagnets, where the comparatively large cooling intervals, $T_{\text{ref}} - T_m \cong 100$ K, and correspondingly slow cooling rates combine to broaden all the structural features.) The data in Fig. 4 represent empirical evidence for a thermal instability in the reentrant phase of a ferromagnetic system, and, as such, provide definitive evidence that this phase satisfies the Fisher-Huse criteria for a spin glass.

We conclude with a few critical remarks on the appli-

cability of the various specific analytical expressions for the relaxation of the remanent magnetization mentioned in the introduction. While the droplet scaling theory of Fisher and Huse,² and the related mesoscopic domain model of Koper and Hilhorst,³ are indeed able to account qualitatively for many of the complex experimental systematics of pure spin-glass relaxation, in terms of a physically appealing picture of domain growth and fragmentation, a fact which motivated the adoption of the overlap-length criterion in the current reentrant investigation, neither offers a satisfactory functional representation of the measured decay. In particular, double-logarithmic plots of $M_R(t)$ versus $\ln t$ for the reentrant data in Fig. 2(a) show *continuous* negative curvature and thus no evidence for an inverse logarithmic decay over any appreciable time interval, as predicted by the Fisher-Huse model² (although the monotonic increase in the magnitude of the local slope with observation time is generally consistent with the Fisher-Huse predictions²). Fits to the Koper-Hilhorst expression (1), plus a constant baseline, were reasonable only in the limit of very short wait times $t_w \leq 60$ s, where the exponential factor in Eq. (1) reduces to a stretched exponential, and deteriorated very rapidly with increasing t_w , as the discrepancy between Eqs. (1) and (4) became progressively more severe, indicating that some of the specific model assumptions relating to domain growth may be unrealistic.

The percolation model of Chamberlin and Haines,⁸ which is also a theory of activated dynamics, but for dispersive excitations within a *fixed* distribution of *finite* domains, is based on such general geometric considerations that it is difficult to appreciate the physical origins of either the aging or temperature-cycling effects within this theoretical framework. Nevertheless, the two model relaxation functions (3) do provide a reasonable description of the isotherms in Figs. 2 and 3, since each is reducible to one of the empirical expressions (4) or (5) in an appropriate limit:⁸ for $C\omega_+ t < 1$, $M_+(t) \rightarrow$ a stretched exponential, while for $C\omega_- t \gg 1$, $M_-(t) \rightarrow$ a power law. In fact, least-squares fits of the ferromagnetic relaxation data in Fig. 2(b) to $M_-(t)$, plus a constant baseline, are indistinguishable in quality from the power-law fits, as illustrated in Fig. 5(c) for the $T = 70$ K isotherm. Table III summarizes the best-fit parameters for all the ferromagnetic isotherms, and the vertical arrow in Fig. 5(c) shows the relaxation time for the average-sized aligned domains, $\bar{\tau}_- \equiv 1/\bar{\omega}_- = [\omega_-^- \exp(-C/\bar{x})]^{-1}$. Within the reentrant phase, the situation is more complex. In the extreme nonequilibrium limit of short wait times [such as the data

TABLE III. Best-fit parameters to $M_0 + M_-(t)$ in Eq. (3).

T_m (K)	t_w (s)	M_0 (10^{-3} emu/g)	M_i (10^{-3} emu/g)	ω_∞^- (s^{-1})	C
65	60	49.40 \pm 0.70	24.10 \pm 0.52	(7.3 \pm 0.2) $\times 10^2$	71.4 \pm 1.0
70	60	61.80 \pm 0.84	27.30 \pm 4.65	(5.9 \pm 0.1) $\times 10^4$	65.1 \pm 1.2
80	60	75.60 \pm 0.88	24.60 \pm 4.29	(7.6 \pm 1.5) $\times 10^5$	69.3 \pm 2.7
90	60	87.20 \pm 1.09	21.20 \pm 3.57	(2.4 \pm 0.6) $\times 10^6$	82.6 \pm 2.0
100	60	89.30 \pm 1.37	19.00 \pm 3.75	(5.9 \pm 1.8) $\times 10^6$	89.9 \pm 1.7
110	60	83.10 \pm 1.27	17.60 \pm 3.08	(1.9 \pm 0.5) $\times 10^7$	96.9 \pm 1.8

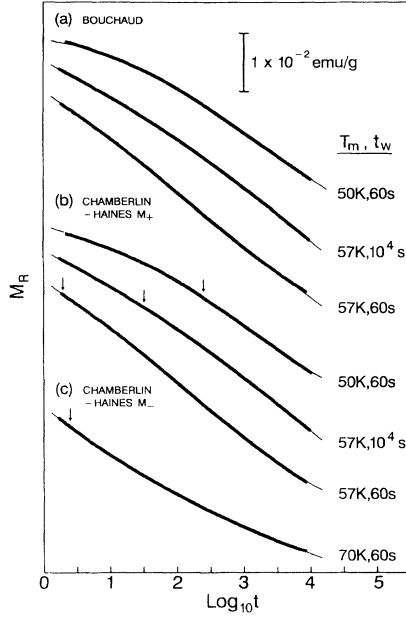


FIG. 5. (a) Some typical fits of the Bouchaud model relaxation function (2) to reentrant isotherms. (b) Some typical fits of the antialigned percolation relaxation function $M_+(t)$ in (3), plus a constant M_0 , to reentrant isotherms. The vertical arrows mark the location of the relaxation time $\bar{\tau}_+$ for average-sized antialigned domains. (c) A typical fit of the aligned percolation relaxation function $M_-(t)$ in (3), plus a constant M_0 , to a ferromagnetic isotherm. The vertical arrow marks the location of the relaxation time $\bar{\tau}_-$ for an average-sized aligned domain.

in Fig. 2(a)], fits to the antialigned function $M_+(t)$ alone, superposed on a constant baseline, are reasonable, but measurably inferior to the stretched exponential ($\ln\chi_+^2/\chi_e^2 \sim 1.1$); however, the quality of these fits improves systematically with increasing system age until, for $t_w \geq 300$ s, the two representations become essentially interchangeable. We interpret this behavior (which would have been unobservable in the Chamberlin-Haines study,⁸ performed at a single, relatively long wait time $t_w = 10^3$ s) as evidence for the inadequacy of a *static* domain-size distribution due to the possibility of domain growth in the early stages of aging. (A six-parameter fit

to a superposition of the aligned and antialigned relaxation functions yields unreliably high parameter uncertainties, and thus reinforces the need to consider the contribution from only one type of domain, at least over the temporal range of this experiment.) Figure 5(b) illustrates fits to $M_+(t)$ at $T_m = 50$ and 57 K, for two extreme wait times $t_w = 60$ s and $t_w = 10^4$ s, and the vertical arrows mark the relaxation time of the average-size antialigned domains, $\bar{\tau}_+ \equiv 1/\bar{\omega}_+ = [\omega_\infty^+ \exp(+C/\bar{x})]^{-1}$, which decreases monotonically with increasing temperature. Table IV provides a complete list of the best-fit parameters for all the reentrant isotherms. The correlation coefficient C increases with temperature, so that, with the physically reasonable assumption of a temperature-independent average interaction between the spins Δ , the percolation correlation length $\xi \propto (\Delta/CT)^\sigma$, where $\sigma = 0.45$ and $\nu = 0.88$ are percolation scaling exponents, decreases with increasing temperature throughout the reentrant phase, which is consonant with its behavior in pure spin glasses.⁸ Thus, a Chamberlin-Haines analysis of the dynamic crossover suggests that the dynamics in the ferromagnetic phase are dominated by domains which are *aligned* with the field, presumably because the reorientation of antialigned domains on field cooling is relatively unhindered in this phase. In the reentrant phase, such antialigned reorientation is inhibited, and the decay is due predominantly to slowly relaxing, higher-energy *antialigned* domains.

The Bouchaud model of thermally activated hopping between metastable, random, free-energy wells postulates a physical mechanism for the aging process, and yields an age-dependent maximum in the relaxation rate $S(t)$ signifying a crossover between two asymptotic relaxation regimes, although it does not directly address the temperature-cycling phenomenon. While the fits to the model expression (2) are consistently a little inferior to the percolation fits in the reentrant regime ($\ln\chi_B^2/\chi_+^2 \sim 0.70$), this model has the property, unique among all the phenomenological models discussed here, of not requiring the “artificial” constant baseline (in fact, the fits are significantly degraded by the inclusion of such a term), and thus may offer the most satisfactory analytical representation of the reentrant and/or spin-glass isotherms, with the fewest variable parameters. Figure 5(a)

TABLE IV. Best-fit parameters to $M_0 + M_+(t)$ in Eq. (3).

T_m (K)	t_w (s)	M_0 (10^{-3} emu/g)	M_i (10^{-3} emu/g)	ω_∞^+ (s^{-1})	C
40	60	119.80±0.08	4.30±0.04	$(2.1 \pm 0.1) \times 10^{-5}$	20.7±0.3
45	60	113.40±0.08	7.00±0.04	$(1.5 \pm 0.1) \times 10^{-5}$	25.4±0.2
50	60	104.60±0.10	11.90±0.07	$(5.4 \pm 0.2) \times 10^{-6}$	37.2±0.3
52	60	100.60±0.05	13.60±0.06	$(6.9 \pm 0.2) \times 10^{-6}$	39.7±0.3
55	60	91.10±0.08	19.90±0.12	$(2.5 \pm 0.1) \times 10^{-6}$	57.9±0.4
57	60	88.60±0.10	26.20±0.22	$(8.0 \pm 0.6) \times 10^{-7}$	78.1±0.8
57	300	89.80±0.10	23.30±0.13	$(9.5 \pm 0.6) \times 10^{-7}$	69.1±0.6
57	900	88.80±0.16	23.00±0.18	$(5.7 \pm 0.4) \times 10^{-7}$	68.8±0.6
57	3 600	85.40±0.31	23.80±0.23	$(1.3 \pm 0.2) \times 10^{-7}$	72.8±0.8
57	10 800	78.80±0.75	25.80±0.44	$(2.0 \pm 0.5) \times 10^{-8}$	80.2±1.2
60	60	85.40±0.16	42.90±0.67	$(4.7 \pm 0.6) \times 10^{-8}$	130.9±2.0

illustrates some typical fits to the model relaxation function (which exhibit deviations similar to those observed by Bouchaud under comparable conditions), and Table V summarizes the best-fit parameters. The parameter x , which provides information on the distribution of free energies in the reentrant and/or spin-glass phase, increases monotonically with temperature and approaches unity as $T \rightarrow 60$ K, which also appears to be the upper limit of stability of the nonequilibrium reentrant phase, thus supporting the random-energy model of Derrida,²³ over the random-exchange SK model.

In summary, we have presented measurements of the low-field thermoremanent decay in a reentrant (Fe, Ni)_{1-x}Mn_x ferromagnet which offer compelling evidence that the reentrant transition actually corresponds to a microscopic collapse of the ferromagnetic spin alignment into an orientationally random, glassy spin configuration. In particular, the equilibrium relaxation dynamics within the high-temperature ferromagnetic phase are replaced, at low temperatures, by a nonequilibrium regime where the relaxation response exhibits a strong dependence on the age of the system, and is compatible with an analytical form commonly used in the representation of pure spin-glass dynamics. More importantly, temperature-cycling experiments clearly confirm the instability of the reentrant phase to arbitrarily small variations in temperature. While this behavior certainly supports the existence of an overlap length scale, which is regarded by theories of mesoscopic domain growth as a defining feature of the spin-glass state, the incompatibility of the specific functional forms predicted by these theories, with the measured decay, prompted compar-

TABLE V. Best-fit parameters to Eq. (2).

T_m (K)	t_w (s)	M_i (10^{-3} emu/g)	γ	x
40	60	131.80±0.01	0.015±0.001	0.29±0.01
45	60	131.70±0.02	0.021±0.001	0.43±0.01
50	60	133.10±0.04	0.029±0.001	0.59±0.01
52	60	133.70±0.06	0.033±0.001	0.69±0.01
55	60	139.80±0.16	0.038±0.001	0.82±0.01
57	60	161.70±0.49	0.038±0.001	0.90±0.01
57	300	165.90±0.36	0.039±0.001	0.91±0.01
57	900	164.00±0.30	0.041±0.001	0.91±0.01
57	3 600	159.80±0.24	0.042±0.001	0.91±0.01
57	10 800	155.50±0.23	0.044±0.001	0.91±0.01
60	60	402.10±5.69	0.042±0.001	0.96±0.01

isons with two other recent models of glassy dynamics based on quite different physical mechanisms. While the quality of the analytical fits is comparable for the two models, the Bouchaud model of random traps appears to be preferable, since it explicitly accommodates the aging process within a more transparent physical framework. However, the origins of the thermal instability have thus far not been addressed within this formalism, and more theoretical work is required in this direction.

ACKNOWLEDGMENT

This work was supported in part by a grant from the Natural Sciences and Engineering Research Council of Canada.

¹L. Lundgren, P. Svedlindh, P. Nordblad, and O. Beckman, *Phys. Rev. Lett.* **51**, 911 (1983).

²D. S. Fisher and D. A. Huse, *Phys. Rev. B* **38**, 373 (1988).

³G. J. M. Koper and H. J. Hilhorst, *J. Phys. (Paris)* **49**, 429 (1988).

⁴C. De Dominicis, H. Orland, and F. Lainée, *J. Phys. Lett. (Paris)* **46**, L463 (1985).

⁵G. Parisi, *Phys. Rev. Lett.* **50**, 1946 (1983).

⁶D. Sherrington and S. Kirkpatrick, *Phys. Rev. Lett.* **32**, 1792 (1975).

⁷J. P. Bouchaud, *J. Phys. I (France)* **2**, 1705 (1992).

⁸R. V. Chamberlin and D. N. Haines, *Phys. Rev. Lett.* **65**, 2197 (1990).

⁹T. C. Lubensky and A. J. McKane, *J. Phys. A* **14**, L157 (1981).

¹⁰B. H. Verbeek, G. J. Nieuwenhuys, H. Stocker, and J. A. Mydosh, *Phys. Rev. Lett.* **40**, 586 (1978).

¹¹A. Wulfes, Ch. Böttger, J. Hesse, J. Sievert, and H. Ahlers, *J. Magn. Magn. Mater.* **104-107**, 2069 (1992).

¹²B. Huck, J. Landes, R. Stasch, and J. Hesse, *J. Phys. (Paris)* **C8, 49**, 1141 (1988).

¹³H. P. Kunkel, R. M. Roshko, W. Ruan, and G. Williams, *Philos. Mag. B* **63**, 1213 (1991).

¹⁴R. D. Barnard, Ch. Böttger, S. Thamm and J. Hesse, *J. Phys. Condens. Matter.* **4**, 7219 (1992).

¹⁵R. Hoogerbeets, W.-L. Luo, and R. Orbach, *Phys. Rev. B* **34**, 1719 (1986).

¹⁶M. Gabay and G. Toulouse, *Phys. Rev. Lett.* **47**, 201 (1981).

¹⁷L. Lundgren, P. Nordblad, and P. Svedlindh, *Phys. Rev. B* **34**, 8164 (1986).

¹⁸P. D. Mitchler, R. M. Roshko, and W. Ruan, *Philos. Mag. B* **68**, 539 (1993).

¹⁹D. A. Huse and D. S. Fisher, *Phys. Rev. B* **35**, 6841 (1987).

²⁰L. C. E. Struik, *Physical Aging in Amorphous Polymers and Other Materials* (Elsevier, Houston, 1978).

²¹C. Rossel, in *Relaxation in Complex Systems and Related Topics*, edited by I. A. Campbell and C. Giovannella (Plenum, New York, 1990).

²²K. Biljakovic, J. C. Lasjaunias, P. Monceau, and F. Lévy, *Phys. Rev. Lett.* **67**, 1902 (1991).

²³B. Derrida, *Phys. Rev. B* **24**, 2613 (1981).